

## Monte-Carlo Simulation Taking Account of Solvent Effects for a Conformation Analysis of Peptides in Solution

Masataka KURODA, Kazuto YAMAZAKI, Tetsu KOBAYASHI,<sup>#</sup> Nobutaka FUJII, and Tooru TAGA\*

Faculty of Pharmaceutical Sciences, Kyoto University, Sakyo-ku, Kyoto 606

(Received October 8, 1993)

Solvent effects were introduced into a Monte-Carlo simulation of peptide conformations by the use of a new potential function for evaluating the nonbonding interactions between solute and solvent molecules. The Monte-Carlo program, which included the electrostatic and nonbonding interactions of the solvent, was tested for a conformation analysis of the zwitterionic tetragastrin in DMSO. The theoretical coupling constants were in good agreement with the NMR data. The conformation of the zwitterion was a folded compact form at the lowest energy, which was different from those obtained from a simulation in vacuo and that without nonbonding solvent effects.

Peptides usually have large flexibility in solution, and it is difficult to determine their characteristic structures, because the energy variation gaps among the different conformations are small. To obtain the most probable conformation in the many local energy minima, we therefore need to carry out careful calculations of the potential energy of the system. When we evaluate the potential energy using semiempirical functions, one of the important factors which must be considered is any solvent effect. The effect of the solvent environment on the conformational stability of a solute molecule has so far been analyzed by several methods.<sup>1)</sup> In this paper, we propose a new potential function for the nonbonding interactions between the solute and solvent molecules, and describe a test of the function in the Monte-Carlo simulations of the conformations of a tetrapeptide named tetragastrin. The results, which were calculated under different solvent conditions, are compared with the NMR data measured in DMSO.

### Potential Functions

A new FORTRAN program for a Monte-Carlo simulation which includes the solvent effects was written. The usual nonbonding, electrostatic, hydrogen-bond, and torsion potential energies were evaluated in the program. The solvent effects were added to these potential energies. The nonbonding potential energy was calculated by the Lennard–Jones 6-12 type function; the used coefficients of the functions were the same as those in ECEPP/2.<sup>2)</sup> The electrostatic energy was calculated using a Coulombic pairwise potential function and the atomic net charges from MOPAC Ver. 6,<sup>3)</sup> which gave more consistent results than that from the net charge of ECEPP/2 in the preliminary computations. The hydrogen-bond energy was calculated using the 10-12 type potential function on the conditions that the proton-acceptor distance be less than 2.5 Å and the proton-donor-acceptor angle be less than 20°.

The interaction energies between the solute and sol-

vent molecules were calculated in two terms of the potential functions. One was the modified Coulomb's potential term, in which the dielectric constant ( $\epsilon$ ) in Eq. 1 was modified,

$$E = q_i q_j / \epsilon R_{ij}, \quad (1)$$

where  $q_i$  and  $q_j$  are the net charges and  $R_{ij}$  is distance between atoms  $i$  and  $j$ . The value of  $\epsilon$  depended on the interstitial distance ( $d_{ij} (= R_{ij} - r_i - r_j)$ ) between atoms  $i$  and  $j$  with the van der Waals radii ( $r_i$  and  $r_j$ , respectively). If  $d_{ij}$  was less than a preset constant ( $r_a$ ),  $\epsilon$  was set to the dielectric constant ( $\epsilon_s$ ) of the solute; if  $d_{ij}$  was larger than the other constant ( $r_b$ ),  $\epsilon$  was replaced by the dielectric constant ( $\epsilon_m$ ) of the solvent. For  $r_a < d_{ij} < r_b$ ,  $\epsilon$  was given by

$$1/\epsilon = 1/\epsilon_m + (1/\epsilon_s - 1/\epsilon_m) \cdot (d_{ij} - r_a) / (r_b - r_a). \quad (2)$$

The second term was a supplemental term for corrections of the lost nonbonded energy due to removing the solvent molecules by the solute molecule. The energy due to this factor is given by the following pairwise function:

$$E(i, j) = w \cdot \{ (V_j/V_s) \cdot E_{sol}(i, j) + (V_i/V_s) \cdot E_{sol}(j, i) \}. \quad (3)$$

$E_{sol}(i, j)$  is the interaction energy between atom  $i$  and a solvent molecule at the position of atom  $j$ .  $V_s$  is the volume of the solvent molecule, and  $V_j$  is the volume of atom  $j$ . Then,  $(V_j/V_s) \cdot E_{sol}(i, j)$  is the effective interaction energy, considering the atomic volume.  $w$  is a function used to evaluate the energy due to removing the solvent molecules from the interspace between atoms  $i$  and  $j$ . If atoms  $i$  and  $j$  were very close based on the condition that  $d_{ij} < r_a$ ,  $w = 1$ . For  $d_{ij} > 2r_s$ ,  $w = 0$ , and for  $r_a < d_{ij} < 2r_s$ ,  $w = 1 - \{ (d_{ij} - r_a) / (2r_s - r_a) \}$ , where  $r_s$  is the van der Waals radius of the solvent molecule.  $E_{sol}(i, j)$  in Eq. 3 was calculated using the 6-12 Lennard–Jones function. The nonbonding energy between atom  $i$  and the solvent atom ( $m$ ) is given by

$$E_{non}(i, j, m) = 1/2 \int_0^\pi (A_{im}/R_{im}^{12} - C_{im}/R_{im}^6) \sin \theta \, d\theta, \quad (4)$$

where  $A_{im}$  and  $C_{im}$  are the van der Waals coefficients,<sup>2)</sup>

<sup>#</sup>Present address: National Institute of Hygienic Sciences, Setagaya-ku, Tokyo 158.

$R_{im}$  the distance between atoms  $i$  and  $m$ , and  $\theta$  the angle made by the vectors from the center of the solvent molecule to the two atoms. If the distance of the atom  $m$  from the molecular center is  $r_{mj}$ , then

$$R_{im} = (R_{ij}^2 + r_{mj}^2 - 2R_{ij}r_{mj} \cos \theta)^{1/2}. \quad (5)$$

Although the center of the solvent molecule was usually fixed at the position of atom  $j$ , if the atom  $j$  became near to atom  $i$ ,  $R_{ij}$  was assumed to be equal to  $r_i + r_s$ .

From Eqs. 4 and 5,

$$Enon(i, j, m) = (FF(r_m/R_{ij}) \cdot A_{im}/R_{ij}^{12} - GF(r_m/R_{ij}) \cdot C_{im}/R_{ij}^6), \quad (6)$$

where  $FF$  and  $GF$  are the fractional polynomial functions given by

$$FF(x) = (1 + 2x^2 + 0.2x^4)(1 + 10x^2 + 5x^4)/(1 - x^2)^{10} \quad (7)$$

and

$$GF(x) = (1 + x^2)/(1 - x^2)^4. \quad (8)$$

If the solvent molecule consisted of  $n$  atoms,  $Esol(i, j) = \sum_m^n Enon(i, j, m)$ .

$$Esol(i, j) = \sum_m^n (FF(r_m/R_{ij}) \cdot A_{im}/R_{ij}^{12} - GF(r_m/R_{ij}) \cdot C_{im}/R_{ij}^6) \quad (9)$$

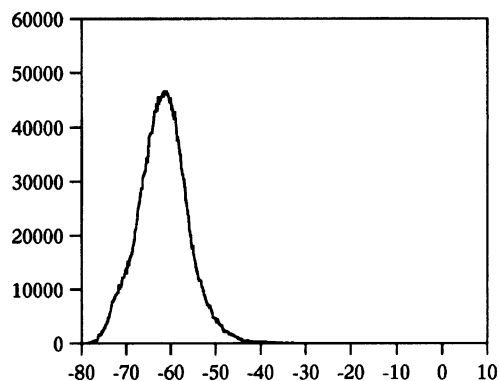
### Method and Procedure

The peptide was assumed to take a zwitterionic form with the ionized N-terminal group ( $-\text{NH}_3^+$ ) and deprotonated carboxyl group of the side chain of Asp<sup>3</sup> ( $-\text{COO}^-$ ). The atomic coordinates of the initial molecular model were fixed in the standard geometry for each amino acid residue. The variables in the model were seventeen dihedral angles of  $\phi$  and  $\psi$  for the main chain and  $\chi$  for the side chain. All of the  $\omega$  angles were set to  $180^\circ$ , and the  $\chi^4$  angle, which determines the rotation of the methyl group of Met<sup>2</sup>, was fixed to an adequate value.

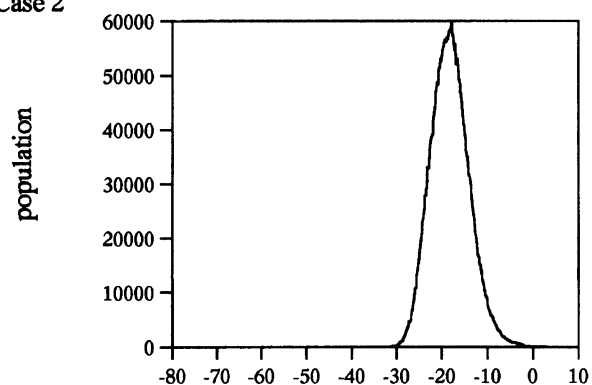
The Monte-Carlo simulation was undertaken using the usual Metropolis algorithm.<sup>4)</sup> One dihedral angle was chosen by random sampling; the value was set from a random number ( $-1$ — $1$ ) multiplied by a prefixed maximum angular transformation value. The energy for the new conformation was then calculated. If the energy was lower than that for the previous conformation, the structure was switched to the new one. If the energy was higher than that for the previous conformation, a random number ( $\eta(0$ — $1)$ ) was compared with the value  $\rho$  of  $\exp(-\Delta E/kT)$ , where  $\Delta E$  is the energy difference between the two conformers, and  $kT$  is the Boltzman temperature factor. If  $\eta$  was higher than  $\rho$ , the structure was kept as the previous one; if  $\eta$  was lower than  $\rho$ , it was replaced by a new one.

In order to achieve effective sampling of the configurations of the peptide chains in multidimensional space, the processes were divided into a number of clusters including three stages: annealing, energy minimizing, and sampling. In the annealing stage,  $\Delta E$  was tentatively reduced by a dumping factor (default value 0.1), and the acceptance of the new

Case 1



Case 2



Case 3

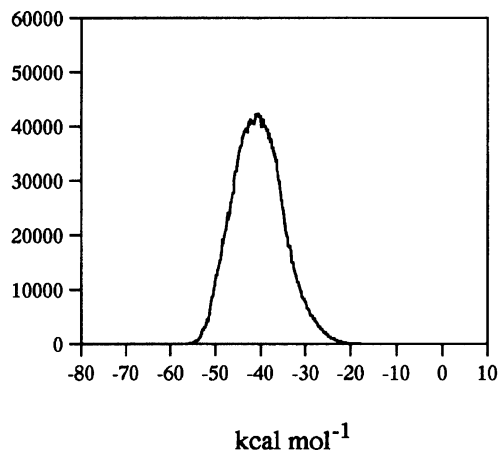


Fig. 1. Energy distributions of the system in MC simulations for three cases: case 1, in vacuo; case 2, including the electrostatic interactions of DMSO only; case 3, including both the electrostatic and nonbonding interactions. (1 cal=4.184 J).

conformation was artificially increased. In the energy-minimizing stage, the structure was converged into that in the local energy minimum. In the sampling stage, the first 500 steps were rejected in order to obtain the energetic equilibrium of the system; the following 1000 steps were used for statistical calculations. In the MC iteration procedures, the first 50 clusters were rejected, and a total of 3000 clusters (including  $3 \times 10^6$  sampling conformers) were calculated.

Three different medium conditions were tested. The first was the vacuo case in which the dielectric constant ( $\epsilon$ ) was

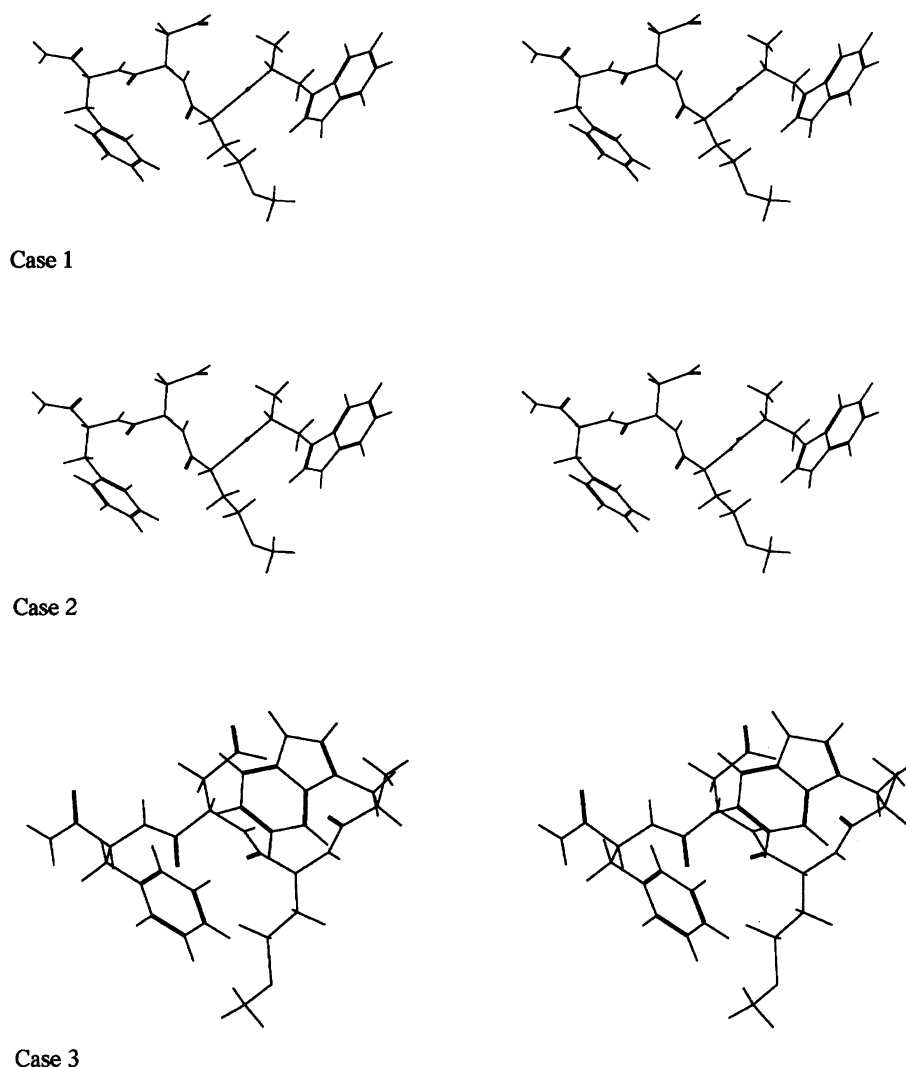


Fig. 2. Stereographic structures in the lowest energy for the three cases.

set to 2.0<sup>5)</sup> and the nonbonding solvent interactions were neglected. The second was the case which included the electrostatic interactions of DMSO, but neglected any nonbonding interactions. The third was the case which fully accounted for the solvent effects, in which both electrostatic and nonbonding interactions were taken account. The dielectric constant ( $\epsilon_m$ ) of DMSO was assumed to be 45.0;  $\epsilon_s$  of the solute was assumed to be 5.0. The preset distances ( $r_a$  and  $r_b$ ) were set to 1.0 and 10.0 Å, respectively.

All of the computations were performed on an IBM RS/6000. One cluster calculation took about 8 s for the vacuo case and 12 s for the case in which the solvent effects were included.

**NMR Measurement.** The peptide was prepared by the solid-phase method of a Fmoc-based peptide synthesis; the major components from the resin were purified by HPLC. The purity of the sample was checked and confirmed by HPLC and <sup>1</sup>H NMR. The pH was adjusted to 6.5 with NaOH aq; after lyophilization, the peptide was dissolved into DMSO-*d*<sub>6</sub>.

The <sup>1</sup>H NMR spectra were measured on Bruker AC-300 and AM-600 spectrometers. The concentration of the pep-

Table 1. Coupling Constants from the Three MC Simulations and the NMR Experiment

		Case1	Case2	Case3	NMR
$J_{\text{HN}\alpha}$	Met <sup>2</sup>	7.8	7.4	7.2	
	Asp <sup>3</sup>	7.6	7.1	6.7	6.7
	Phe <sup>4</sup>	7.9	8.0	8.0	8.1
$J_{\alpha\beta}$	Trp <sup>1</sup>	6.3	6.1	6.8	5.3
		8.2	8.5	8.3	7.9
	Met <sup>2</sup>	6.0	6.3	6.7	5.3
		9.9	9.4	9.1	8.3
	Asp <sup>3</sup>	5.3	5.9	5.8	6.2
		9.5	9.0	9.5	7.9
	Phe <sup>4</sup>	7.4	7.3	6.5	4.4
		8.2	8.3	9.3	9.2

tide was 4.9 mol m<sup>-3</sup> in DMSO-*d*<sub>6</sub>. The assignment of the proton peaks relied on COSY<sup>6)</sup> and NOESY.<sup>7)</sup> The coupling constant ( $J_{\text{HN}\alpha}$ ) of each residue was obtained from the 1D-

Table 2. Theoretical and Experimental Existence Probabilities of Three Rotamers about  $\chi^1$  Rotation from the MC Simulation for the Case 3 and the NMR Experiment

Rotamer		Case 3 <sup>a</sup> /%	NMR <sup>b</sup> /%
Trp <sup>1</sup>	gg	37.7	41.1
	gt	41.8	42.0
	tg	20.5	16.9
Met <sup>2</sup>	gg	6.3	37.2
	gt	31.8	16.9
	tg	61.9	45.9
Asp <sup>3</sup>	gg	28.3	32.4
	gt	22.9	25.6
	tg	48.8	42.0
Phe <sup>4</sup>	gg	15.9	37.2
	gt	23.5	8.2
	tg	60.6	54.6

a) gg, gt, tg are referred to the  $\chi^1$  angles 0–120°, 120–240°, and 240–360°, respectively. b) Each population was calculated by the method in Ref. 11. The gt and tg rotamers were distinguished by the method in Ref. 12 using the NOE intensities.

Table 3. Dihedral Angles for the Three Conformers in the Lowest Energy

		Case1	Case2	Case3
Trp <sup>1</sup>	$\psi$	146	159	-173
	$\chi^1$	60	62	80
	$\chi^2$	79	94	-71
Met <sup>2</sup>	$\phi$	49	52	-87
	$\psi$	49	37	94
	$\chi^1$	-67	-68	-168
Asp <sup>3</sup>	$\chi^2$	-179	-174	178
	$\chi^3$	-166	-175	-165
	$\phi$	-84	-75	-77
Phe <sup>4</sup>	$\psi$	156	157	160
	$\chi^1$	-45	-56	-55
	$\chi^2$	-91	-69	3
Phe <sup>4</sup>	$\phi$	-150	-138	-134
	$\psi$	150	157	141
	$\chi^1$	-61	60	-54
	$\chi^2$	109	104	117

spectra, and  $J_{\alpha\beta}$  was obtained from E. COSY.<sup>8)</sup>

### Results and Discussion

The state numbers vs. the energy values in the three simulations are given in Fig. 1. The distributions are normal for all cases and the simulations were adequately undertaken. The dispersions of the energy distributions are 31.0, 17.6, and 30.6 for cases 1, 2, and 3 respectively.

The values of the coupling constants ( $J_{\text{HN}\alpha}$  and  $J_{\alpha\beta}$ ) were calculated by applying the Karplus equation for each case,<sup>9,10)</sup> and then compared with the observed values given in Table 1. The  $J_{\text{HN}\alpha}$  of Met<sup>2</sup> could not be observed because of a broadening of its amide proton signal. The values of  $J_{\text{HN}\alpha}$  for case 3, fully evaluating

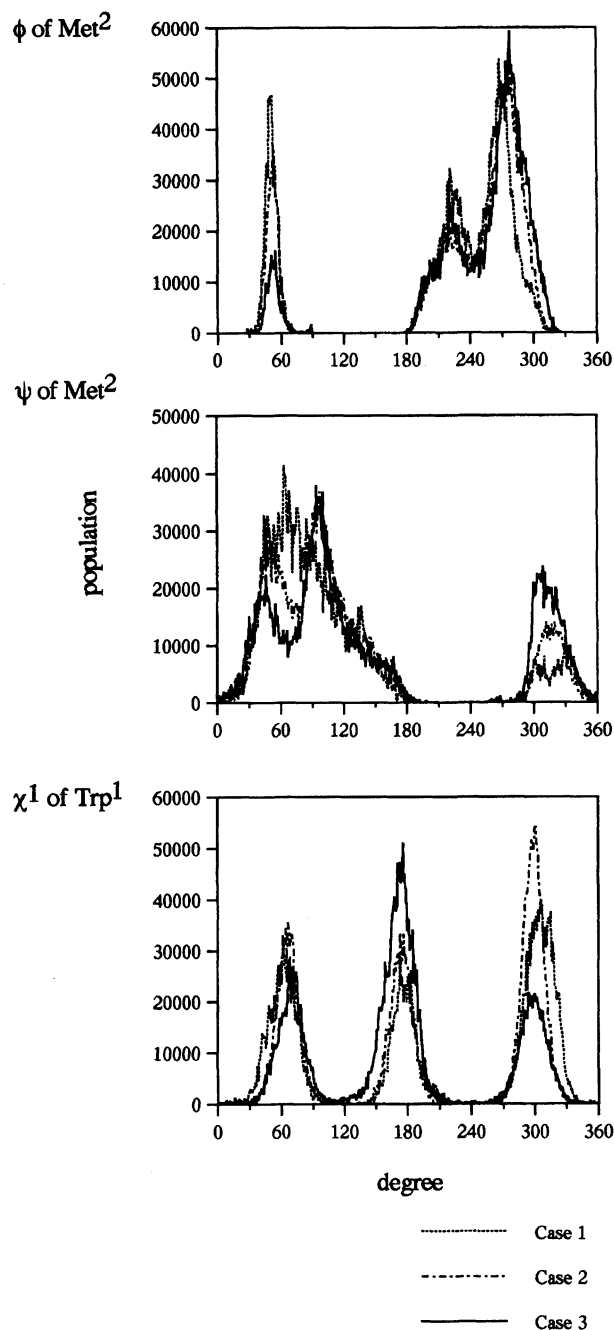


Fig. 3. The  $\phi$  and  $\psi$  distributions for Met<sup>2</sup> and the  $\chi^1$  distribution for Trp<sup>1</sup> for the three cases.

the solvent effects, show excellent agreement with the observed values. The values of  $J_{\alpha\beta}$  for case 3 are also relatively closer to the NMR values than those for the others. For case 3, the probabilities of three idealized conformations (gg, gt, and tg) around the  $\text{C}_\alpha\text{--C}_\beta$  bond were evaluated from the  $\chi^1$  distributions. The theoretical probabilities, except for gg of Met<sup>2</sup> and gt of Phe<sup>4</sup>, are in good agreement with those from the NMR experiment, as given in Table 2; gt of Trp<sup>1</sup> and tg of the other three residues are major conformations in both theory and experiment.

Table 3 lists the dihedral angles of the structures in the lowest energy state for the three cases. Figure 2 illustrates the stereographic models for the three structures. The structures for cases 1 and 2 have a similar extended form, whereas the structure for case 3 is different. For all of the structures, although hydrogen bonds are not formed, the O<sub>δ</sub> of Asp<sup>3</sup> is close to the amino N of Trp<sup>1</sup> with distances of 3.5—4.3 Å. The aromatic rings of Trp<sup>1</sup> and Phe<sup>4</sup> of the structures for cases 1 and 2 are apart by distances of 12.0 and 12.6 Å between the centers of the rings, respectively. On the other hand, the two rings of the structure for case 3 are close together at a distance of 5.2 Å. Though the main chain was as extended as that of the other two structures, the total conformation of the last one was relatively compact compared with the two close aromatic rings.

As shown in Fig. 3, the  $\phi$  and  $\psi$  distributions for Met<sup>2</sup> and the  $\chi^1$  distribution for Trp<sup>1</sup> depend on the treatment of solvent effects. For case 3, the  $\phi$  distribution at around 50° is large, the  $\psi$  distribution at around 310° is small, and the  $\chi^1$  distribution has a main peak at 180°. These distributions indicate that the major conformers in DMSO are folded structures with a helix conformation at the Met<sup>2</sup> and with two close aromatic rings. The structure is close to that of the lowest energy.

As described so far, the different treatments of the solvent effects in the energy calculations result in different statistic distributions of the conformers as well as different structures of the low-energy conformations. It is therefore important to consider the solvent effect in order to simulate what occurs in a liquid medium. In the present test, the simulation using the new proposed function for evaluating the solvent effects gave the best agreement regarding the coupling-constant values between theory and experiment, and also gave consistent

results for the molecular structure from the NMR experimental data. In conclusion, the potential function proposed here was proved to be useful for an energy evaluation of the system in the solvent.

## References

- 1) e. g., a) R. B. Hermann, *J. Phys. Chem.*, **76**, 2754 (1972); b) D. L. Beveridge, M. M. Kelly, and R. J. Radna, *J. Am. Chem. Soc.*, **96**, 3769 (1974); c) R. R. Birge, M. J. Sullivan, and B. E. Kohler, *J. Am. Chem. Soc.*, **98**, 358 (1976); d) I. Tvaroska, *Biopolymers*, **21**, 1887 (1982); e) T. Ooi, M. Oobatake, G. Némethy, and H. A. Scheraga, *Proc. Natl. Acad. Sci. U. S. A.*, **84**, 3086 (1987).
- 2) F. A. Momany, L. M. Carruthers, R. F. McGuire, and H. A. Scheraga, *J. Phys. Chem.*, **78**, 1595 (1974).
- 3) J. J. P. Stewart, *QCPE Bull.*, **9**, 10 (1989).
- 4) N. Metropolis, A. W. Rosenbluth, M. N. Rosenbluth, A. H. Teller, and E. Teller, *J. Chem. Phys.*, **21**, 1087 (1953).
- 5) F. A. Momany, R. F. McGuire, A. W. Burgess, and H. A. Scheraga, *J. Phys. Chem.*, **79**, 2361 (1975).
- 6) W. P. Aue, E. Bartholdi, and R. R. Ernst, *J. Chem. Phys.*, **64**, 2229 (1976).
- 7) J. Jeener, B. H. Meier, P. Bachman, and R. R. Ernst, *J. Chem. Phys.*, **71**, 4546 (1979).
- 8) C. Griesinger, O. W. Sørensen, and R. R. Ernst, *J. Magn. Reson.*, **75**, 474 (1987).
- 9) A. Pardi, M. Billeter, and K. Wüthrich, *J. Mol. Biol.*, **180**, 741 (1984).
- 10) M. T. Cung and M. Marraud, *Biopolymers*, **21**, 953 (1982).
- 11) J. Feeny, G. C. K. Roberts, J. P. Brown, A. S. V. Burgen, and H. Gregory, *J. Chem. Soc., Perkin Trans. 2*, **1972**, 601.
- 12) G. Wagner, W. Braun, T. F. Havel, T. Schaumann, N. Gö, and K. Wüthrich, *J. Mol. Biol.*, **196**, 611 (1987).